The Multiple Sweep Method of Moments (MSMM) Design of Wide-Band Antennas

D. Çolak and E. H. Newman, *Fellow, IEEE*

***Abstract*— This paper presents the use of the multiple sweep method of moments (MSMM) in the design of electrically large wide-band antennas. The MSMM is an $\mathcal{O}(N^2)$ recursive method for solving the large matrix equations which arise in the method of moments (MM) analysis of electrically large bodies. Although the MSMM is a frequency-domain solution, it has a time-domain interpretation. The main point of this paper is to show that this time-domain interpretation can be used to identify the location and magnitude of points of current reflections, thus making the MSMM a useful tool for analysis and design of wide-band antennas. The method is applied to the three-dimensional (3-D) problems of a long dipole antenna with a reactive load in the center of each arm and a TEM horn antenna with a bend.**

I. Introduction

In the design of electrically large wide-band antennas one generally wants a structure which permits the current to flow from the generator onto the antenna surfaces with as little reflection as possible. The frequency-domain method of moments (MM) has been one of the most reliable and widely used numerical methods for the analysis of antennas of simple or complex shape [1]–[6]. In the MM the current on a body is expanded in terms of N expansion functions, and the N unknown coefficients in this expansion are obtained as the solution of an order N matrix equation. The standard MM has two main limitations. The first is associated with the fact that the number of unknowns N in the MM solution is proportional to the electrical size of the antenna and, thus, the MM is often limited by the $\mathcal{O}(N^3)$ CPU time required to solve the MM matrix equation by direct methods such as LU decomposition. By contrast, the multiple sweep method of moments (MSMM) [7]–[9] requires $\mathcal{O}(N^2)$ CPU time. The second limitation is a result of the fact that, although the MM can provide extremely accurate results for the antenna current distribution, it provides no insight into the mechanisms which affect the antenna current. Thus, with the standard MM it is extremely difficult to relate a computed current distribution to the physical features of the antenna. The main point of this paper is to show that the MSMM has a simple time-domain interpretation, which can identify points of current reflection and thus provide valuable design insight. It will further be shown that the MSMM has the ability to analyze a small section of the antenna in an isolated fashion, thus minimizing the CPU time for a parameter study to optimize the geometry of that section.

Over the past several years many methods have been developed to improve the computational efficiency of the MM, and thus allow it to be applied to electrically larger bodies [10]. Recently, the authors described a technique termed the multiple sweep method of moments (MSMM) [7]–[9], which can reduce the matrix solution time to $\mathcal{O}(N^2)$ (or less if it is combined with the fast multipole method [11]–[16]). The MSMM is an extension or modification of the spatial decomposition technique (SDT) developed by Umashankar *et al*. [17]. In both methods the electrically large body is split into P sections containing approximately N/P unknowns per section. The currents on the P sections are found in a recursive fashion until they (hopefully) converges to the exact result. When applied to antennas, the main difference between the MSMM and the SDT is that the MSMM views the time harmonic voltage source as a step function which turns on at time $t = 0$. The MSMM procedure then attempts to follow the current as it flows out of the generator onto the antenna arms. The first sweep accounts for first order reflections of the current, while subsequent sweeps account for higher order reflections. Tapered resistance cards [18]–[23] are used on the first sweep to isolate first order reflections of the current and to remove unphysical reflections at the ends of the sections. Subsequent sweeps are performed in the order in which currents change with time, so that the higher order sweeps correspond to higher order reflections of the current. Although there is no proof or guarantee of convergence of the MSMM, previous results [7]–[9] indicate that for low Q wide-band antennas, the MSMM converges to engineering accuracy in only a few sweeps.

Section II of this paper presents the MSMM solution for a symmetric two-arm antenna, and in particular, it is shown how the previously presented MSMM procedure [7]–[9] can be modified to include an interior point of reflection. A reflection coefficient for each MSMM section is defined which can be used to locate and assess the strength of points of reflection. In Section III, the procedure is applied to a three-dimensional (3-D) TEM horn antenna, while Section IV presents the MSMM design procedure. Finally, Section V describes the major advantages of the MSMM, as compared to the standard MM, in the design of electrically large wide-band antennas. All of the MM computations in this paper were made with the *Electromagnetic Surface Patch Code* which employs a piecewise sinusoidal solution of the electric field integral equation [24].

Manuscript received February 13, 1997; revised June 25, 1998. This work was supported by the Joint Services Electronics Program, The Ohio State University Research Foundation under Contract N00014-78-C-0049.

The authors are with the ElectroScience Laboratory, The Ohio State University, Columbus, OH 43212 USA.

Publisher Item Identifier S 0018-926X(98)07056-2.

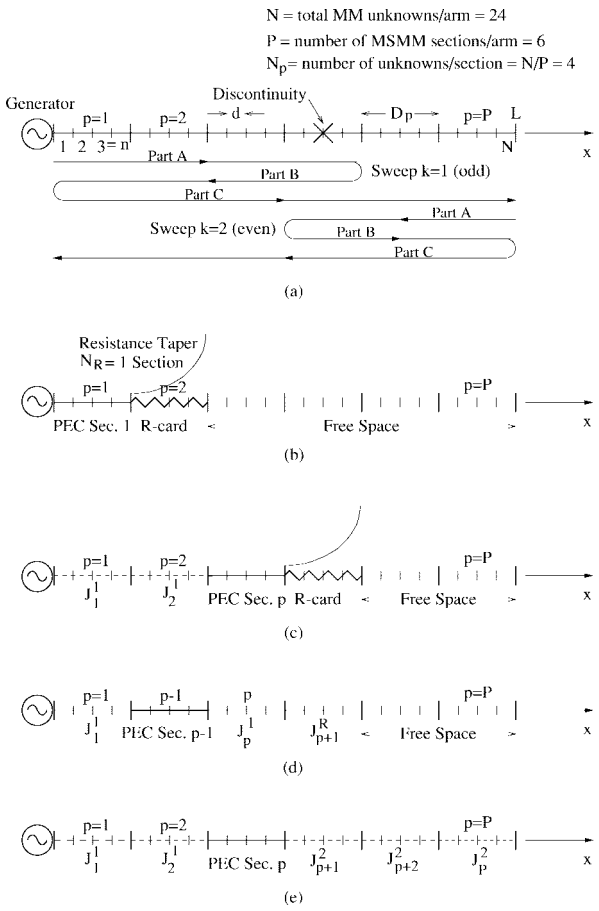

Fig. 1. For the MSMM solution antenna Arm 1 of length L is split into P sections with $N_p = N/P$ unknowns per section. (a) MSMM Sweeps $k = 1$ and 2 on dipole Arm 1. (b) Computation of J_1^1 = Sweep 1 current on section $p = 1$. (c) Computation of J_p^1 = Sweep 1 current on section p. (d) Computation of $\bar{J}_{p-1}^1$ =Modified Sweep 1 current on section p-1. (e) Computation of J_p^2 =Sweep 2 current on section p.

II. The MSMM Solution for a Two-Arm Antenna

A. Geometry for the MM and MSMM Solution

This section illustrates the application of the MSMM to a perfect electric conducting (PEC) symmetric two-arm antenna. Fig. 1(a) symbolically shows one arm of the symmetric center-fed antenna of total length $2L$. The excitation is by a unit amplitude time-harmonic voltage source. As indicated by the heavy $\times$, there may be a point of discontinuity or reflection in each arm. Although the antenna in Fig. 1(a) is pictured as a straight-arm dipole, the reader should note that the arms could be curved to form a spiral or helix antenna, or even expanded in width to form a horn antenna.

For the purposes of the standard MM solution, each arm of the antenna is split into N segments of width $d = L/N$ and the symmetric $\hat{\mathbf{x}}$ directed current is expanded as

$$J(x) = \sum_{n=1}^{N} i_n J_n(x) \quad \text{on Arm 1: } x \geq 0 \\ + \sum_{n=1}^{N} i_n J_n(-x) \quad \text{on Arm 2: } x \leq 0. \tag{1}$$

where the J_n are the known basis functions and the i_n are the unknown current coefficients. Employing the MM procedure, the unknown coefficients from (1) can be found as the solution of the order $2N$ matrix equation

$$\begin{bmatrix} [Z^{1,1}] & [Z^{1,2}] \\ [Z^{2,1}] & [Z^{2,2}] \end{bmatrix} \begin{bmatrix} I \\ I \end{bmatrix} = \begin{bmatrix} V \\ V \end{bmatrix} \tag{2}$$

where the $Z^{i,j}$ are order N impedance matrices, which account for mutual coupling between basis and weighting functions on Arms $i, j = 1, 2$, V is the reaction between the antenna voltage generator and the basis functions on Arms 1 and 2, and $I = [i_1, i_2, \cdots, i_N]^T$ is the current vector which holds the unknown coefficients on Arms 1 and 2.

For the purposes of the MSMM solution, each arm of the antenna is split into P equal sections of approximately $N_p = N/P$ expansion functions per section and of approximate width $D_p = L/P$[1]. The sweep $k = 1, 2, \cdots, \infty$ current on arm 1 section $p = 1, 2, \cdots, P$ is denoted

$$J_p^k = \sum_{n=(p-1)N_p+1}^{pN_p} i_n^k J_n \tag{3}$$

and similarly $J_{p'}^k$ denotes the current on arm 2 section p'. The sweep k current vector is denoted $I^k = [i_1^k, i_2^k, \cdots, i_N^k]^T$.

B. The First Sweep

Although the MSMM is not rigorously a time-domain solution, it is helpful to visualize it as computing the time-domain antenna current due to a step function time-harmonic voltage source, $v_s(t) = \exp(j\omega t)u(t)$, which turns on at time $t = 0$. The $k = 1$ or first sweep will track the current as it first propagates from the generator to the ends of the antenna, and will include only first order reflections of the current. The first sweep begins by computing the current, $J_{p=1}^{k=1}$ and $J_{p'=1}^{k=1}$ on arm 1 section $p = 1$ and arm 2 section $p' = 1$ caused by the generator when it first turns on. At this point, the remaining sections $p, p' \geq 2$ have no current, thus creating unphysical discontinuities and reflections of the antenna current at the ends of sections $p, p' = 1$. As illustrated in Fig. 1(b), to minimize these unphysical reflections, the outer edges of sections $p = 1$ and $p' = 1$ are terminated in tapered R cards. The resistance smoothly tapers from zero at the inner edge to a very large resistance at the outer edge. For convenience, we always choose the width of the R cards to be an integer number, N_R, of sections. For simplicity in Fig. 1 and in the discussion to follow, we will assume an $N_R = 1$ section R card. Thus, sections $p = p' = 1$ are PEC, sections $p = p' = 2$ are tapered R cards, and the remaining sections are free-space. Once the current on sections $p = p' = 1$ has been determined, the next step is to compute the current on sections $p = p' = 2$ caused by the generator plus the previously computed currents on section 1. The process is continued until all of the sweep 1 currents have been computed.

[1] Due to the use of *overlapping* piecewise sinusoids, there is not a one to one correspondence between the MM segments and the MM basis functions. This small difference in numbering is ignored in this paper. In general, MSMM sections should be viewed as groups of basis functions and not as physical sections of the body.

Consider the computation of the first sweep current, $J_p^{k=1}$ and $J_{p'}^{k=1}$, on arbitrary arm 1 section p and arm 2 section p'. As illustrated in Fig. 1(c), sections 1 to $p-1$ on arm 1 and sections 1 to $p'-1$ on arm 2 contain previously computed sweep 1 currents, sections p and p' are PEC, the next $N_R = 1$ sections on each arm are tapered R cards, and the remaining sections are free-space. Note that no tapered R card is needed at the inner edges of sections p and p' since the previously computed currents on sections $p-1$ and $p'-1$ (approximately) enforce continuity of current at the junction and, thus, from an electromagnetic viewpoint there is no edge. The currents on PEC sections p and p' and R card sections $p+1$ and $p'+1$ are produced by the superposition of the voltage generator plus the previously computed currents on sections 1 to $p-1$ and 1 to $p'-1$ radiating in the presence of PEC sections p and p' and R card sections $p+1$ and $p'+1$. Assuming that the antenna has no points of reflection, then sweep $k=1$ continues until the current on all sections $p, p' = 1, 2, \cdots, P$ have been computed. Note that when computing the current on the last sections $p = p' = P$, no R card is used since the outer edge is a real termination of the antenna.

If there is a point of reflection on the antenna arms, then it must first be detected, and then the MSMM procedure is modified so that sweep $k=1$ includes first order reflections of the current. To detect reflections, each time we compute the current on sections p and p', we recompute the current on the previous sections $p-1$ and $p'-1$. As illustrated in Fig. 1(d), the recomputed current on section $p-1$, denoted $\tilde{J}_{p-1}^1$, is the current induced on PEC section $p-1$ by the source, the previously computed sweep $k=1$ currents on sections 1 to $p-2$ and p, plus the previously computed current on the R-card section $p+1$. We then define the reflection coefficient for section p as

$$R_p = \frac{\left\| \tilde{J}_{p-1}^1 - J_{p-1}^1 \right\|}{\left\| \tilde{J}_{p-1}^1 \right\|}. \tag{4}$$

If $J_{p-1}^1 \approx \tilde{J}_{p-1}^1$ then R_p is small and there is little or no reflections in section p. In this case the MSMM procedure continues to larger p, p' out the antenna arms. However, if R_p exceeds some threshold value, then as indicated at the $\times$ in Fig. 1(a), the MSMM procedure reverses direction and follows the reflected current back toward the generator, at which point it again reverses and proceeds out the antenna arms. When it again reaches the discontinuity it does not reverse again since this would correspond to a second-order reflection of the current and sweep 1 only includes first-order reflections. Sweep 1 proceeds out past the discontinuity until either it reaches the end of the antenna or a second discontinuity is reached. This out to the reflection point, back to the generator and out again to the end process is denoted parts A, B, and C in Fig. 1(a). If a second discontinuity is detected, the MSMM procedure reverses inward toward the generator and then proceeds back out the antenna arms. In doing this, it does not reverse at the first discontinuity since doing so would correspond to a second-order reflection of the current.

Fig. 2 illustrates the ability of the MSMM to detect a point of reflection. The insert shows a dipole antenna of arm length

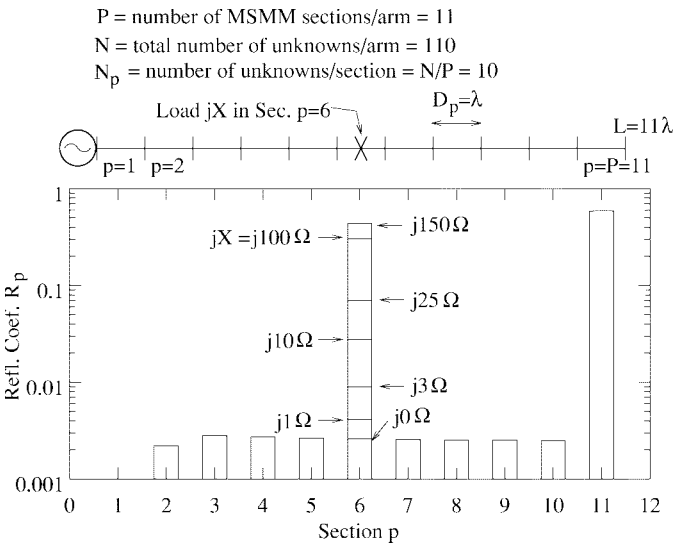

Fig. 2. The reflection coefficient for a reactive load jX in sections $p = 6$ of a dipole antenna.

$L = 11\lambda$ and with $N = 110$ MM expansion functions per arm. For the MSMM solution each arm is segmented into $P = 11$ sections of width $D_p = L/P = 1\lambda$ and with $N_p = N/P = 10$ unknowns per section. A reactive load jX is placed at the center of each arm of the dipole, i.e., at the center of MSMM sections $p = p' = 6$. Fig. 2 shows the reflection coefficient, R_p, for sections $p = 2, 3, \cdots, P = 11$, and for various values of the reactive load jX. Note that (except for the last section which has a near unity reflection coefficient) for the MSMM sections that do not have the load, the reflection coefficient is small, and on the order of 0.003. This sets a noise or threshold value for the smallest reflection which can be detected. As illustrated in Fig. 2, a load of $j1\ \Omega$ corresponds to a reflection coefficient of $R_6 \approx 0.004$ and is just above the threshold. As jX increases, R_6 increases and the point of reflection in sections $p = p' = 6$ is easily detected.

The MSMM can identify the location of the points of reflection to a resolution on the order of the MSMM section size $D_p = L/P$, which suggests the use of many small MSMM sections. By contrast, assuming an $N_R = 1$ section R cards, the main limitation on the noise or threshold value for the reflection coefficient is the ability of the R card section to act as perfect absorbers. As $D_p = L/P$ increases, the R cards become better absorbers and the noise or threshold level for the reflection coefficients decrease. Also, the convergence of the MSMM typically improves as D_p increases [7]–[9]. As a compromise between these factors, D_p should typically be chosen on the order of a wavelength.

For the dipole with a load of $jX = j100\ \Omega$, Figs. 3(a)–(c) show a comparison between the MSMM sweep $k=1$ and the exact MM current. Part A starts at the generator section $p=1$ and shows no indication of a reflection (i.e., no ripple) until it gets to the load section 6. Part B reverses inward toward the generator and begins to approximate the ripple in the exact MM current. Finally, Part C goes from the generator to the last section $p = P = 11$. Sections $p > 6$ show no ripple until the currents gets to the last section $p = P = 11$.

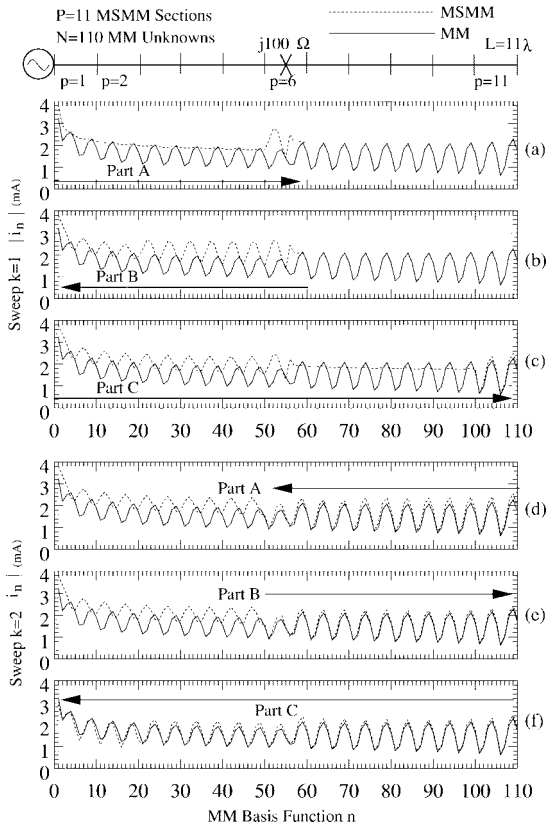

Fig. 3. A comparison of the exact MM and MSMM current for (a)–(c) sweep $k = 1$ and (d)–(f) sweep $k = 2$.

C. The Second and Subsequent Sweeps

At the conclusion of the first sweep the antenna current is known to first order in reflections, and the MSMM sections, which contain points of reflection have been identified. The second sweep improves the accuracy of the current by including reflections to order 2. As illustrated in Fig. 1(a), the second sweep is done in reverse order since this is the natural order in which the currents would change with time. As was the case for sweep $k = 1$, sweep $k = 2$ is done in the three Parts A, B and C.

Fig. 1(e) illustrates the computation of the sweep $k = 2$ current on arbitrary sections p and p', i.e., $J_p^{k=2}$ and $J_{p'}^{k=2}$. In computing the sweep 2 current on sections p and p', sections p and p' are PEC, while all other sections are represented by their most recently computed currents. Focusing on arm 1, at this point in the sweep 2 computation, sections $p+1$ to P have already been updated to the sweep 2 currents, while sections 1 to $p-1$ still have the sweep 1 currents. No resistance cards are needed since J_{p-1}^1 and J_{p+1}^2 approximately enforce continuity of current at the left and right edges of section p, respectively (except for section P which has a real edge). The current on sections p and p' is the superposition of that due to the voltage generator plus all previously computed currents. It has been found that the accuracy and convergence of the MSMM can be improved by also allowing sections $p-1$ and $p'-1$ to be PEC [9].

All sweeps $k > 2$ are identical to sweep 2, except that odd numbered sweeps proceed outward from the generator, while even numbered sweeps proceed inward from the ends as the MSMM solution attempts to model multiple reflections of the current.

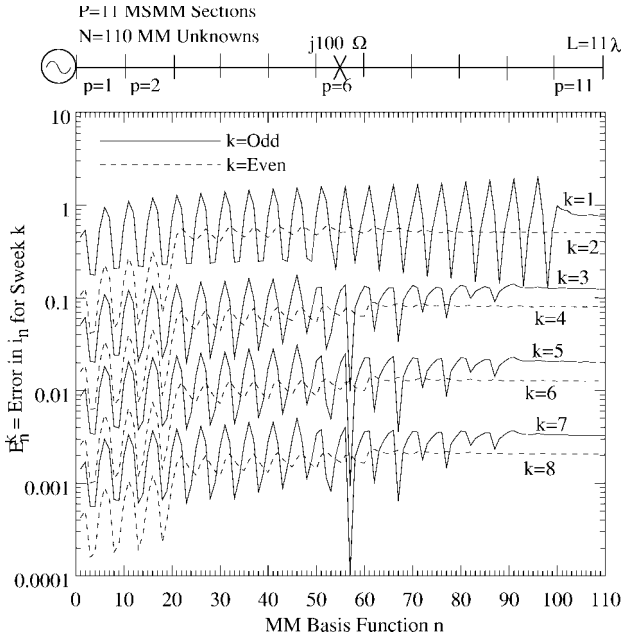

Fig. 4. $E_n^k =$ the error for basis function n on sweep k.

Fig. 3(d)–(f) show a comparison of the sweep $k = 2$ MSMM current and the exact MM current. Part A proceeds from the last section $p = 11$ to the load section $p = 6$. It is considerably better than the sweep $k = 1$ current since it includes the effects of reflection at the ends of the dipole. Part B proceeds from the load section 6 back to the end section 11 and is a noticeable improvement over Part A. Finally, Part C proceeds from the end section 11 to the generator section 1 and yields a current which is probably adequate for most engineering applications.

The error in computing the current coefficient for basis function n on sweep k is

$$E_n^k = \frac{|\mathrm{MM}\, i_n - \mathrm{MSMM}\, i_n|}{|\mathrm{MM}\, i_n|} \quad \text{on sweep } k. \tag{5}$$

For the same dipole as Figs. 3, Fig. 4 shows E_n^k versus MM basis function n, and for sweeps $k = 1, 2, \cdots, 8$. Note that two sweeps produce a monotonic decrease in the error for (almost) every current coefficient.

Now define the total root mean square (rms) error for sweep k as

$$\text{RMS Error} = E^k = \frac{\sqrt{\sum_{n=1}^{N} |\mathrm{MM}\, i_n - \mathrm{MSMM}\, i_n|^2}}{\sqrt{\sum_{n=1}^{N} |\mathrm{MM}\, i_n|^2}}. \tag{6}$$

Fig. 5 shows the rms error for sweeps $k = 1$ to 30. The solid line is for the MSMM procedure shown in Fig. 1(a) consisting of Parts A, B and C, while the dashed line is for the old MSMM procedure consisting of Part C only [7]–[9]. Note that the new MSMM procedure converges to essentially machine accuracy in about 13 sweeps, while the old MSMM

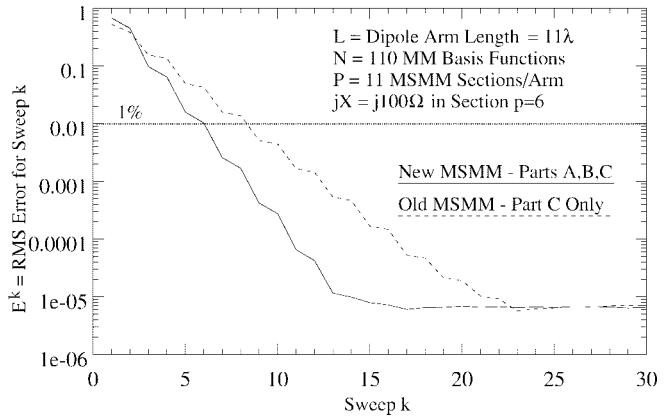

Fig. 5. E^k = the RMS error for sweep k.

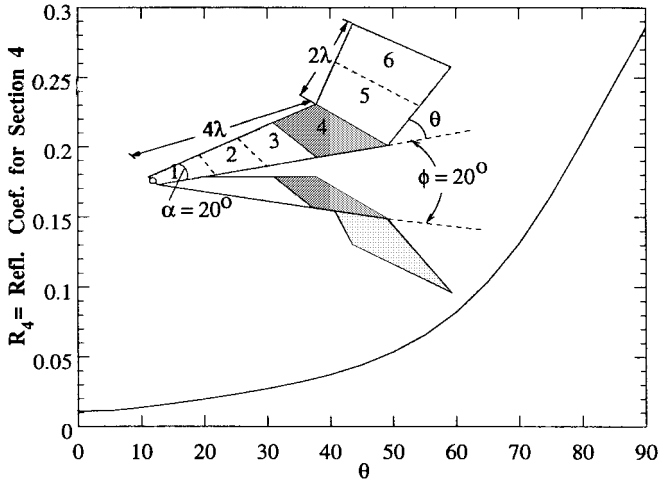

Fig. 6. Reflection coefficient at the discontinuity of a TEM horn antenna.

procedure requires about 23 sweeps. More importantly, the new MSMM procedure converges to engineering accuracy of 1% in just six sweeps. Further, previous results indicate that the convergence of the MSMM improves as the electrical size of the body increases.

III. TEM Horn Antenna

Fig. 6 shows a TEM horn antenna [25] which we view as a center-fed symmetric two-arm antenna. Each arm consists of a nearly triangular plate whose width expands with angle $\alpha = 20°$ as one moves out the antenna arms. The total arm length is 6λ and a bend of angle θ at distance 4λ from the generator will produce a reflection of the current. Since the two arms are at an interior angle of $\phi = 20°$, the bent plate is vertical when $\theta = 80°$. For the purposes of the MSMM solution each arm is split into $P = 6$ MSMM sections, and the bend is at the end of section $p = 4$ (and $p' = 4$). To illustrate the ability of the MSMM to detect the discontinuity, Fig. 6 shows R_4 = the reflection coefficient for section $p = 4$ versus the angle θ. When $\theta = 0$, i.e., no discontinuity, R_4 is about 0.01. However, as θ increases, R_4 increases, and the discontinuity can be detected.

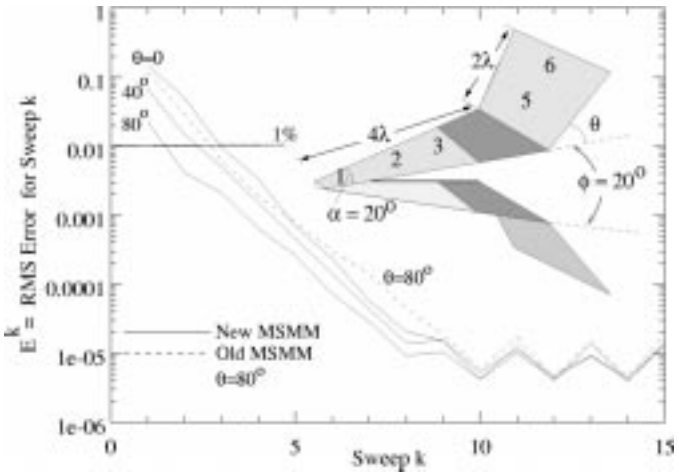

Fig. 7. Convergence of the MSMM solution for a TEM horn antenna.

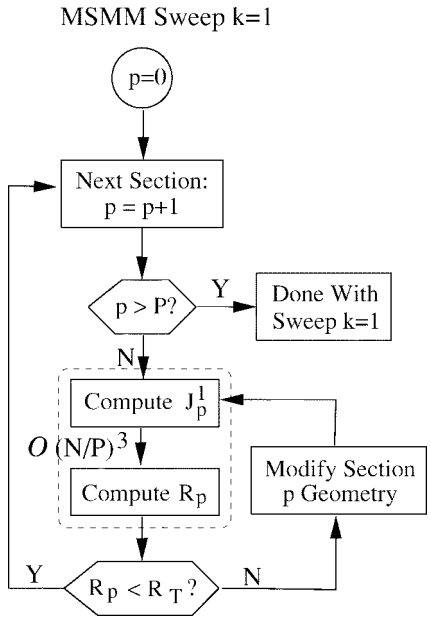

Fig. 8. MSMM sweep 1 design procedure.

Fig. 7 shows the convergence of the MSMM solution for horns of angle $\theta = 0°$, $40°$, and $80°$. For $\theta = 80°$ the dashed line shows the old MSMM procedure which does not include the out-back-out sweep of Fig. 1(a). Note that on the early sweeps the new out-back-out MSMM sweep improves the accuracy by almost an order of magnitude, however, the old and new methods eventually converge to the same values. Also, in all cases the MSMM procedure converges to an engineering accuracy of 1% in three sweeps or less.

IV. MSMM Design Procedure

This section describes a procedure for designing a wide-band antenna with minimum CPU time using the MSMM. With the MSMM the antenna is designed, i.e., its geometry is determined, on the $k = 1$ or first sweep since this is when the points of reflection are identified. As indicated by the flow chart of Fig. 8, MSMM sweep 1 begins by computing

the current, J_p^1, and reflection coefficient, R_p, for sections $p = 1, 2, \cdots, P$ moving from the generator out the antenna arms. Each time a reflection coefficient is computed it is compared to some small threshold level denoted R_T.

If $R_p < R_T$, then the reflections in section p are considered negligible, and the MSMM procedure continues to larger p out the antenna arms.

If $R_p \geq R_T$ then the reflections in section p are considered to be too large, and some change to the geometry of section p is required. The antenna engineer modifies the section p geometry, and then recomputes only J_p^1 and R_p. Note that it is not necessary to restart the procedure at section $p = 1$, since the sweep $k = 1$ currents on sections 1 to $p - 1$ do not depend on the geometry of section p. The new R_p is compared to R_T, and the process is continued until a modification to the section p geometry is found such that $R_p < R_T$.

Note that each time the geometry of section p is changed the MSMM requires the solution of a relatively small order $N_p = N/P$ system of equations. Following the three part procedure of Fig. 1(a), the MSMM should now reverse direction to Part B inward toward the generator, and then proceed outward on Part C. In practice this complexity is probably not warranted since $R_p < R_T$ is small, and thus at this point sweep 1 is simply continued outward until either another reflection greater than the threshold is found or the end of the antenna arms are reached.

V. Conclusion

This paper has described the applications of the MSMM to the design of wide-band antennas. As compared to the standard MM, the MSMM has three important advantages. First, by computing the reflection coefficient, R_p, for each section the MSMM can assess the strength and locate points of reflection to a resolution of the MSMM section size, D_p. By contrast, the MM provides no simple way to relate the computed current to the geometry of the antenna. Second, the MSMM is extremely efficient in performing a parameter study to modify the geometry of the antenna to improve its performance. With the MSMM design procedure of Fig. 8, one modifies the geometry of section p, and then solves an order $N_p = N/P$ system of equations for the current on section p, J_p^1. This requires $\mathcal{O}(N/P)^3$ solve time. By contrast, with the standard MM any change in the geometry requires the computation of the entire current vector by the solution of an order N system of equations, requiring $\mathcal{O}(N^3)$ solve time. Thus, even for a modest size body with $P = 10$, each iteration in the design procedure can be $P^3 = 1000$ times faster with the MSMM. The final advantage of the MSMM is that it provides a definite method for determining whether or not a geometry change is helpful, since it allows the engineer to study the discontinuities in an isolated fashion one at a time. A change to the geometry of section p only changes R_p, and thus if R_p decreases the change is deemed good. By contrast, with the standard MM one must analyze the global geometry which may contain several discontinuities which interact with each other in a complicated manner. This makes it very difficult to assess whether a particular change in the geometry is good or bad. The primary disadvantages of the MSMM are that it is difficult to apply to an arbitrarily shaped body, and that convergence of the method is not guaranteed. However, even if the MSMM does not converge, sweep 1 can still be used to identify and minimize points of reflection.

References

[1] R. F. Harrington, *Field Computation by Moment Methods*. Malarbar FL: Krieger, 1982.

[2] R. F. Harrington, "Matrix methods for field problems," in *Proc. IEEE*, vol. 55, pp. 136–149, Feb. 1987.

[3] E. K. Miller, L. Medgyesi-Mitschang, and E. H. Newman, *Computational Electromagnetics—Frequency-Domain Method of Moments*. New York: IEEE Press, 1992.

[4] R. C. Hansen, *Moment Methods in Antennas and Scattering*. Boston, MA: Artech, 1990.

[5] J. J. H. Wang, *Generalized Moment Methods in Electromagnetics*. New York: Wiley, 1991.

[6] E. K. Miller, "A selective survey of computational electromagnetics," *IEEE Trans. Antennas Propagat.*, vol. 36, pp. 1281–1305, Sept. 1988.

[7] D. Torrungrueng, E. H. Newman, and W. D. Burnside, "The multiple sweep method of moments (MSMM) analysis of electrically large bodies," in *IEEE Antennas Propagat. URSI Meet.*, Baltimore, MD, July 1996, p. 25.

[8] D. Torrungrueng, "The multiple sweep method of moments (MSMM) analysis of electrically large bodies," M.Sc. thesis, Ohio State Univ., Columbus, OH, June 1996.

[9] D. Torrungrueng and E. H. Newman, "The multiple sweep method of moments (MSMM) analysis of electrically large bodies," *IEEE Trans. Antennas Propagat.*, vol. 45, p. 1252, Aug. 1997.

[10] E. H. Newman and I. Tekin, "An overview of the method of moments analysis of large systems," in *Nat. Res. Council Symp. Large-Scale Structures*, Washington, DC, Sept. 1994, pp. 204–220.

[11] W. D. Murphy, V. Rokhlin, and M. S. Vassilou, "Acceleration methods for the iterative solution of electromagnetic scattering problems," *Radio Sci.*, vol. 28, pp. 1–12, Jan./Feb. 1993.

[12] V. Rokhlin, "Rapid solution of integral equations of classical potential theory," *J. Computat. Phys.*, vol. 60, pp. 187–207, 1983.

[13] V. Rokhlin, "Rapid solution of integral equations of scattering theory in two dimensions," *J. Computat. Phys.*, vol. 86, pp. 414–439, 1990.

[14] N. Engheta, W. D. Murphy, and V. Rokhlin, "The fast multipole method (FMM) for electromagnetic scattering problems," *IEEE Trans. Antennas Propagat.*, vol. 40, pp. 634–641, June 1992.

[15] R. J. Burkholder and D.-H. Kwon, "High-frequency asymptotic acceleration of the fast multipole method," *Radio Sci.*, vol. 31, pp. 1199–1206, Sept./Oct. 1996.

[16] J. Song, C.-C. Lu, and W. C. Chew, "Multilevel fast multipole algorithm for electromagnetic scattering by large complex objects," *IEEE Trans. Antennas Propagat.*, vol. 45, pp. 1488–1493, Oct. 1997.

[17] K. R. Umashankar, S. Nimmagadda, and A. Taflove, "Numerical analysis of electromagnetic scattering by electrically large objects using spatial decomposition technique," *IEEE Trans. Antennas Propagat.*, vol. AP-40, pp. 867–877, Aug. 1992.

[18] L. N. Medgyesi-Mitschang and J. M. Putman, "Integral equation formulation for imperfectly conducting scatterers," *IEEE Trans. Antennas Propagat.*, vol. AP-33, pp. 206–214, Feb. 1985.

[19] E. H. Newman and J. L. Blanchard, "TM scattering by an impedance sheet extension of a parabolic cylinder," *IEEE Trans. Antennas Propagat.*, vol. 36, pp. 527–534, Apr. 1988.

[20] T. B. A. Senior and J. L. Volakis, "Sheet simulation of a thin dielectric layer," *Radio Sci.*, vol. 22, pp. 1261–1272, Dec. 1987.

[21] R. F. Harrington and J. R. Mautz, "An impedance sheet approximation for thin dielectric shells," *IEEE Trans. Antennas Propagat.*, vol. 23, pp. 531–534, July 1975.

[22] T. B. A. Senior, "Backscattering from resistive strips," *IEEE Trans. Antennas Propagat.*, vol. AP-27, pp. 808–803, Nov. 1979.

[23] E. H. Newman and M. R. Schrote, "An open surface integral formulation for electromagnetic scattering by material plates," *IEEE Trans. Antennas Propagat.*, vol. AP-32, pp. 672–678, July 1984.

[24] E. H. Newman, "A user's manual for the electromagnetic surface patch code: ESP version IV," ElectroSci. Lab. Rep. 716199-11, Ohio State Univ., prepared under Grant NSG 1498 with NASA, Langley Res. Ctr., Hampton, VA, Aug. 1988.

[25] M. Kanda, "Transients in a resistively loaded linear antenna compared with those in a conical antenna and a TEM horn," *IEEE Trans. Antennas Propagat.*, vol. AP-28, pp. 132–136, Jan. 1980.

Dilek Çolak was born in Aksehir, Turkey in 1970. She received the B.S. and M.S. degrees in electrical engineering from Bilkent University, Ankara, Turkey, in 1991 and 1993, respectively. She is currently working toward the Ph.D. degree from The Ohio State University ElectroScience Laboratory, Columbus.

Her research interests are in the areas of electromagnetic wave theory and applications and especially computational techniques.

Ms. Çolak was a recipient of the Young Scientist Award of the International Union of Radio Science (URSI) at the 24th General Assembly in 1993.

E. H. Newman, (S'67–M'74–SM'86–F'89) for a photograph and biography, see p. 1258 of the August 1997 issue of this TRANSACTIONS.